CONTROLLABLE STATIC BREATH-FIGURE PROCESSES TO FORM ORDERED 3-D MICROSTRUCTURES ON POLYDIMETHYLSILOXANE WITHOUT LITHOGRAPHY AND MOLDING

*Junce Cheng and Tingyi "Leo" Liu**
University of Massachusetts Amherst, MA, USA

ABSTRACT

We report a one-step lithography-free molding-free method to create highly-ordered hexagonally-packed 3-D micro-cavities on a soft polymeric material using a controllable static breath-figure formation process. To study the key control parameters that are missing in the existing literature for breath figure formation, we designed and built a system to monitor the real-time microscopic condensations at the under-curing polymeric interface with synchronous temperature measurement of water vapor and polymer interface altogether. Such a multimodal sensing system enabled us, for the first time, to visualize the entire breath figure formation process and correlate it to several key parameters to control the formation of breath figures.

KEYWORDS

Breath figure, 3-D microstructure, soft material, PDMS, molding-free, lithography-free, highly-ordered

INTRODUCTION

Breath figures are found in our daily lives whenever water vapor in the air condensates on a cold substrate, e.g., the fog on the cold window when a human breathes nearby, such as Figure 1(a). This simple phenomenon attracts great interest in research because the condensed water droplets may reorganize themselves via energy minimization and orientate into a highly ordered hexagonally-packed honeycomb configuration. If water droplets are condensed on a polymer fluid that is under curing, the polymer may be solidified with surface structures with the water condensates working as microscale molds, as depicted in Figure 1 (b).

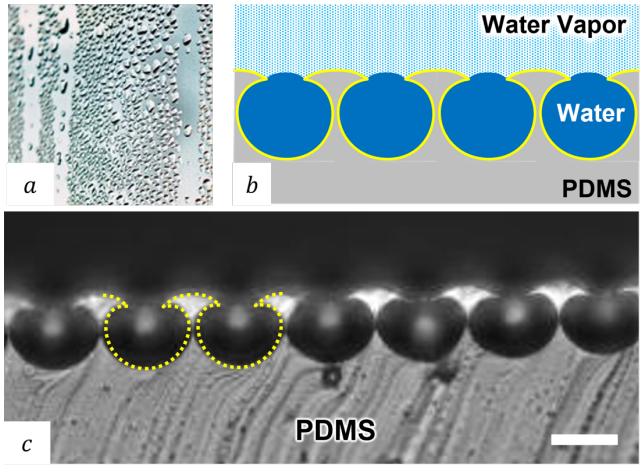

Figure 1: (a) Breath figure found in daily lives where tiny water droplets condensate on a cool aluminum substrate and self-orientate into an ordered dense pattern. (b) Schematic of breath figures formed at the interfaces of liquid PDMS in a humid environment. (c) An optical microscope image of the cross-section of the breath figure structures that were created on PDMS using the method described in this report. The scale bar is 10 μm.

Figure 1 (b) shows an example of this kind of process where the polymer under curing is an elastomer, polydimethylsiloxane (PDMS) [1]. Provided a humid environment, water drops can condense on the cool surface of an uncured PDMS, partially immersing in the PDMS and functioning as a molecularly smooth 3-D micro mold that can be easily removed by evaporating the water droplet once the PDMS is cured, as shown in Figure 1 (c). The well-ordered hexagonally packed breath figures also provide a unique opportunity to create hollow/porous structures and periodic patterns on various polymers that are mostly rigid [2-8]. Overall, the formation of breath figures shows great potential for surface patterning without going through the traditional MEMS processes [9]. Unlike usual micromanufacturing, breath-figures processes do not require a cleanroom setting to obtain micro- and nano-patterns through photolithography, resulting in a low-cost, time-efficient, and simple fabrication. Albeit all the potential advantages listed above, however, almost all of the reported breath figure formation processes were case-to-case successes capable of producing specific breath figures patterns from a particular polymer. This is because there exists a complicated coupled heat transfer relationship between water condensation and evaporation, resulting in the key parameters to obtain controllable breath-figure patterns are not well understood and thus success is largely obtained by trial and error. Therefore, in order to utilize breath figures for manufacturing, we need a better understanding of the underlying mechanisms with quantification of the key parameters contributing to the formation of various breath figures.

Current techniques to form breath figure patterns include dynamic processes [10] and static processes [1] that are highly specific to the processing polymers. In dynamic processes, a water vapor flow is dynamically controlled to maintain the vapor humidity in the process chamber. By tuning the humidity, the outcome breath figures were monitored and studied to help understand the underlying mechanisms [13]. However, due to the uncertainties caused by flow disturbance, the dynamic processes are difficult to repeat, resulting in inconsistent breath figures from process to process. Furthermore, the success of dynamic processes has been restricted to nonelastic polymers where the rigid plastics were dissolved in a volatile solvent that is more suspectable to evaporation than water. The breath figures are formed when both the solvent and water are evaporated. This method may not work for thermally cured elastomers because, rather than purely evaporating the solvent, most elastomers are formed via thermal curing with the development of covalent crosslinks where water droplets may be evaporated before elastomers are cured. The static processes, on the other hand, have been shown to realize breath figure patterns in a more consistent and repeatable manner, as well as on soft elastomers under curing. For example, static processes of uniform hexagonal breath figures formation on polydimethylsiloxane (PDMS) have been reported [1], showing great potential for soft materials patterning applications. However, the underlying mechanism of the breath figures formation in a closed heated container is unclear [1] due to the complicated multi-parameters heat transfer relationship between water condensation and evaporation and the lack of direct visualization in previous experiments [1]. In this paper, we will monitor the real-time temperature and images of breath figure

978-1-940470-04-7/HH2022/$25©2022TRF
DOI 10.31438/trf.hh2022.57

formation with a controllable static process to get a better understanding of the mechanisms behind this static breath figure formation process. Understanding the key controllable parameters like the cooling effect by changing the different supporting materials will help elucidate some of the underlying mechanisms. The existence of various adjustable parameters (e.g., PDMS base to curing agent ratio, PDMS volume, temperature etc.) gives us ample room to dictate the process and generate unique breath-figure patterns for various applications.

THEORY

While the mechanism to form controllable breath figures is somehow unclear, the requirements of water droplets to nucleate and grow on the under-curing polymer due to condensation is beyond question. When hot water vapor in the air encounters a cool liquid pool, water droplets will nucleate on the cool interface, as shown in Figure 2(a), becoming the water condensate required to form breath-figure patterns [3, 14]. Given the sufficiently small water droplets in this nucleation state, the force balance analysis is performed considering only the interfacial forces due to negligible gravitational effect compared to surface tensional effect at this scale. The force or stress balance is given in the two equations below:

$$\sigma_{12} \sin\theta_{12} = \sigma_{13} \sin\theta_{13} \quad (1)$$

$$\sigma_{23} \sin\theta_{13} = \sigma_{12} \sin(\theta_{12} + \theta_{13}) \quad (2)$$

where "1" is water, "2" is PDMS, and "3" is water vapor in our case. For the static breath figures formation process we studied in this report, water, PDMS, and air are put in an enclosed chamber, as shown in Figure 2 (b). In the beginning, the cooling water evaporates by heat, and then water vapor nucleates on the top of the cooling PDMS surface. Then water droplets increase the size because the speed of water condensation is faster than the speed of water evaporation at the interface of liquid water and vapor. Ratios of dimensions of water droplets maintain nearly the same although the surface tensions of water, PDMS, and vapor change slightly with temperature. During the growth of water droplets and crosslinking of PDMS, water droplets assemble themselves as islands in the hexagonal array that rarely merge or collapse [10]. However, the energy balance of assembly and merging is still under research. At the end of the process, PDMS cures completely and becomes warm. Water evaporates and leaves small openings (i.e., mouth) on the top of the PDMS film. Dictated by the interfacial tension between fluids 1, 2, and 3, these openings can be relatively small compared to the size of the cavities embedded in the bulk (e.g., PDMS).

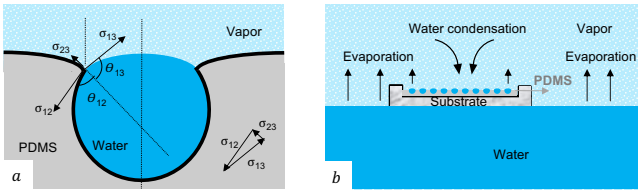

Figure 2: Mechanisms of breath figure: (a) Nucleation of water droplets on a cool PDMS liquid pool under curing. Water droplets are balanced by interfacial tensions at the three-phase interface. The stress at the three-phase interface can be represented by the Neumann triangle (shown in the bottom right corner). (b) In an enclosed heated container, water may serve as the vapor source for condensation while providing cooling to the substrate to induce condensation of water droplets on the liquid PDMS. The balance between the evaporation and condensation heat transfer is the key to forming breath figures in this static process, which is the focus of the current paper.

EXPERIMENTS

To get a better understanding of the mechanisms behind this static breath figure formation process, we designed a real-time multimodal sensing system for the characterization of the formation of breath figure patterns at the top surface of the polymer. Figure 3 shows the schematic of our experimental setup. The real-time visualization of water condensates on the top PDMS surface was monitored by a modular microscope imaging system (VIS vertical Mitutoyo widefield video microscope unit) with a long-working distance lens (20× Mitutoyo Plan Apo SL infinity corrected objective). The real-time temperature monitoring of water vapor and PDMS substrate was realized by the feedthrough connection of two thermocouples (RTD-805 air temperature RTD sensor from Omega Engineering and BB-IM-C08-M3 K-type surface thermocouple sensor from Biaobiao) across the oven (set as 50°C) to measure the temperature at multiple locations inside the enclosed container. Both thermocouples were connected to a data acquisition board (National Instruments NI CompactDAQ 9211) that recorded data at a rate of 4 samples/s. PDMS (Sylgard™ 184) was used as the experimental soft polymer to characterize the formation of breath figure patterns on elastomers. The mixing ratio of the PDMS part A:B (i.e., base vs. curing agent) was fixed at 5:1 in all of our experiments. We poured the degassed PDMS mixture into a holder made of a piece of silicon wafer (as the high thermal conductive substrate) and PDMS walls (to hold the liquid PDMS). The enclosed container has a transparent plastic cover for direct monitoring of condensation and thin metallic walls for conducting the heat from the oven to water to create water vapor.

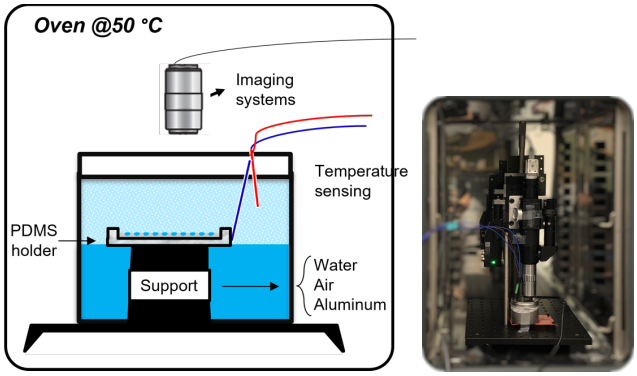

Figure 3: Experimental setup for real-time monitoring breath figure formation. The schematic on the left shows the setup and the picture on the right shows the actual setup built inside a convective oven with sensing and imaging signals feedthrough to NI DAQ and a computer outside the oven. The oven temperature was set to 50°C to slowly heat up the water inside the sealed container and cure the PDMS. The temperature of the water vapor and PDMS holder were measured by thermocouples fed through the container. An imaging system composed of the long-working-distance objective lens and a digital camera was set up to monitor the real-time condensation of water droplets on the under-curing PDMS surface.

To investigate the cooling effect on breath figure formation, the liquid PDMS was supported by three different materials, i.e., water, air, and aluminum, with very different thermal properties. The related heat transfer properties of these supporting materials are summarized in Table 1 together with the experimental breath figure patterns formed on PDMS. Synchronous condensation monitoring and temperature measurements were conducted for these three different supports to study their correlation to the breath figures.

Table 1. Summary of the thermal properties of the materials (water, air, and aluminum) that support the under-curing PDMS, the corresponding top view of the experimental breath figures, and their cross-sectional schematics.

	Water	Air	Aluminum
Thermal conductivity coefficients ($W \cdot m^{-1} \cdot K^{-1}$)	0.598	0.029	239
Isobaric mass heat capacity ($J \cdot g^{-1} \cdot K^{-1}$)	4.181	1.004	0.897
Thermal diffusivity (mm^2/s)	0.143	19	97
Resultant breath figures (top view)	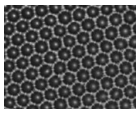		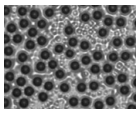
Cross section			

RESULTS AND DISCUSSION

Figure 4 shows the temperature curve of water vapor and the under-curing PDMS fluid. Initially, the temperature of water vapor increased more rapidly than the temperature of under-curing PDMS because air/vapor had a higher thermal diffusivity than water by which liquid PDMS was cooled. This generated a growing temperature difference between the water vapor and liquid PDMS, leading to faster water condensation over evaporation on the liquid PDMS, and thus resulting in water droplets formed on liquid PDMS and breath figures formation. Once the temperature of water vapor was close to the set temperature of the oven, it maintained at this highest temperature while the liquid PDMS temperature kept increasing from oven heating, causing the temperature difference between water vapor and liquid PDMS to become smaller so that water evaporation may be dominating over condensation during the curing of fluidic PDMS.

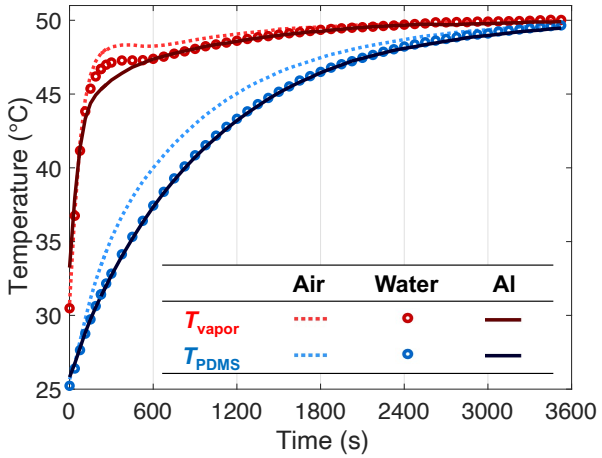

Figure 4: Temperature curves of water vapor (red) and the under-curing PDMS substrate (blue) monitored inside the enclosed container. Three different supports have been studied in this report: air (dots), water (circles), and aluminum (solid lines).

Figure 4 showed the images of breath figure formation on PDMS with different supporting materials in time sequences. In the first 60 seconds, water started to nucleate on the surface of liquid PDMS. The temperature difference was also nearly the same with different supporting materials according to Figure 4. Then, water droplets started to grow and self-orientate in different morphologies. If we sort the area between temperature curves of water vapor and PDMS (i.e., integration of temperature difference over time), the ascending order with an increasing area will be air supports, aluminum supports, and water supports, which is related to the phenomena shown in Figure 4. The breath figures were sparsely packed when the PDMS holder was supported by aluminum while breath figures were found to form shallow cavities (i.e., little water embedded in PDMS) when the PDMS holder was supported by air. Around 1400 seconds later, the morphologies of the top surface of PDMS were fixed, indicating that water condensation and migration are done with droplets reaching the maximum dimensions.

Combining information from Table 1, Figure 4, and Figure 5, we found that (1) while water and aluminum supports had almost overlapping temperature curves after 400 seconds, they showed a major difference around ~200-300 seconds. Such difference reduced the water condensation on the aluminum supported sample so that it did not have enough water droplets to self-orientate to form ordered patterns; (2) while water and air supports produced a similar top view of ordered water droplets, the low thermal conductivity of air prevents sufficient cooling from the water underneath the PDMS under-curing and thus causing a faster temperature increase of the under-curing liquid PDMS. This may result in early PDMS curing before water droplets were embedded in the liquid PDMS. While water droplets could continue to condensate and migrate on top of the increasingly viscous PDMS and evaporate completely in the end, they can no longer be embedded inside the PDMS and thus only produce very shallow cavities.

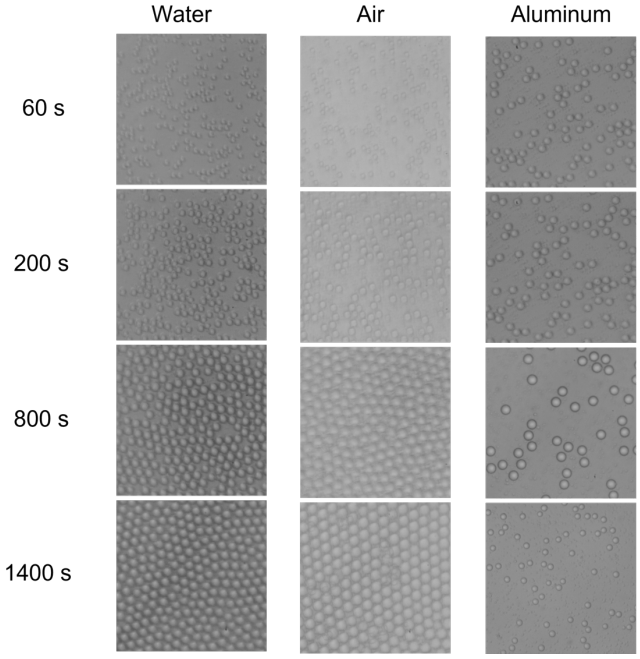

Figure 5: The time series images of breath figure formation on PDMS with different supporting materials. Water allows sufficient condensation and re-organization to form ordered breath figure patterns while the air support created ordered but very shallow patterns and the aluminum support created sparse water condensate. Each figure represents an area of 167 × 167 μm^2.

Using water as the support, highly-ordered breath figure patterns were successfully formed and cured on PDMS with confirmed SEM micrographs, as shown in Figure 6 with both the angled view and cross-section confirming the formation of breath figures. Our sample had a ~3-µm top open mouth and a ~14-µm diameter cavity. The yield of the highly-ordered pattern was ~90% in a 1 inch^2 area. The breath figure patterns assembled as cavity islands where neighboring cavities did not interconnect with each other, similar to other reports such as [10]. Despite of our control experimental study on thermal properties of various supporting materials, there remain many parameters that will affect the level of ordering and surface morphologies of the hexagonally-packed patterns. For example, the viscosity of PDMS fluid, the temperature difference between initial and final conditions, and the thermal properties of the coolant.

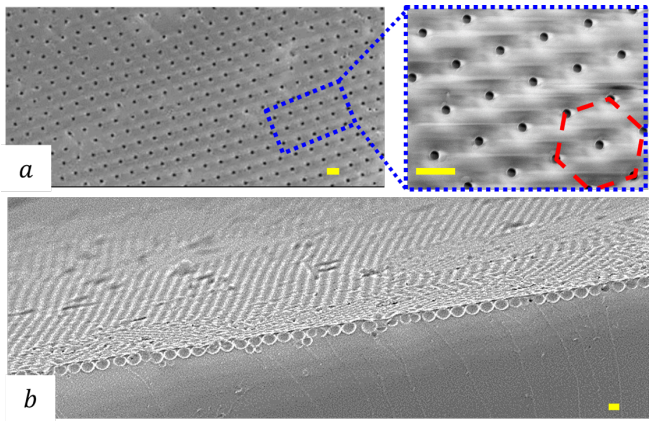

Figure 6: SEM images of breath figure pattern formed by PDMS with crosslinking ratio of 5:1. (a) top view; (b) cross-section view. Scale bars are all 10 µm.

CONCLUSIONS

In this work, we have presented a simple method to create 3-D microstructures on a soft elastomeric material (PDMS) controlled by a static breath figure process. To better understand the underlying mechanism, we have created a multimodal sensing system to simultaneously measure the vapor and liquid temperatures and record optical images of water condensation. Free of lithography and molding/demolding, this method provides an easy yet powerful way to obtain true 3-D microstructures on soft polymeric materials that are difficult to create with traditional MEMS processes. We foresee that the ability to form overhanging (i.e., re-entrant) microstructures without the difficulty of demolding will enable a wide range of applications in super-repellent surfaces, BioMEMS, and wearable devices, etc.

ACKNOWLEDGMENTS

This project is supported by Prof. T. Leo Liu's startup funds provided by the University of Massachusetts Amherst.

REFERENCES

1. S. Shojaei-Zadeh, S. R. Swanson, and S. L. Anna, Highly uniform micro-cavity arrays in flexible elastomer film, *Soft Matter,* 5. 4, (2009).
2. D. Beysens and C. M. Knobler, Growth of Breath Figures, *Physical Review Letters,* 57. 12, (1986).
3. C. M. Knobler and D. Beysens, Growth of Breath Figures on Fluid Surfaces, *Europhysics Letters (EPL),* 6. 8, (1988).
4. A. Steyer *et al.*, Two-dimensional ordering during droplet growth on a liquid surface, *Physical Review B,* 42. 1, (1990).
5. D. Beysens *et al.*, How does dew form?, *Phase Transitions,* 31. 1-4, (1991).
6. A. Steyer, P. Guenoun, and D. Beysens, Hexatic and fat-fractal structures for water droplets condensing on oil, *Physical Review E,* 48. 1, (1993).
7. D. Beysens, The formation of dew, *Atmospheric Research,* 39. 1, (1995).
8. D. Beysens, Dew nucleation and growth, *Comptes Rendus Physique,* 7. 9, (2006).
9. A. Zhang, H. Bai, and L. Li, Breath Figure: A Nature-Inspired Preparation Method for Ordered Porous Films, *Chemical Reviews,* 115. 18, (2015).
10. M. Srinivasarao *et al.*, Three-Dimensionally Ordered Array of Air Bubbles in a Polymer Film, *Science,* 292. 5514, (2001).
11. X. Li, X. Yu, and Y. Han, Polymer thin films for antireflection coatings, *Journal of Materials Chemistry C,* 1. 12, (2013).
12. H. T. Ham *et al.*, Macroporous Polymer Thin Film Prepared from Temporarily Stabilized Water-in-Oil Emulsion, *The Journal of Physical Chemistry B,* 110. 28, (2006).
13. L. Song, Study of Ordered Macroporous Polymer Films by Templating Breath Figures, (2005).
14. A. A. Nepomnyashchy *et al.*, Nucleation and growth of droplets at a liquid-gas interface, *Physical Review E,* 74. 2, (2006).

CONTACT

Prof. T. Leo Liu: Tel: +1 (413) 577-0927; leoliu@umass.edu